Heliyon 9 (2023) e18324

Contents lists available at ScienceDirect

Heliyon

journal homepage: www.cell.com/heliyon

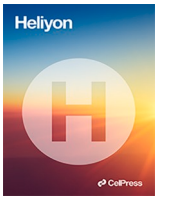

Insights gained from single-cell RNA analysis of murine endothelial cells in aging hearts

Zhong Liu [a,b,1], Yanjing Huang [a,1], Dongliang Wang [a], Mengke Li [a], Qikai Zhang [a], Caineng Pan [a], Yuheng Lin [a], Yuanting Luo [a], Zhuoxing Shi [a], Ping Zhang [a,**], Yingfeng Zheng [a,b,*]

[a] State Key Laboratory of Ophthalmology, Zhongshan Ophthalmic Center, Sun Yat-sen University, Guangdong Provincial Key Laboratory of Ophthalmology and Visual Science, Guangzhou, 510060, China
[b] Research Unit of Ocular Development and Regeneration, Chinese Academy of Medical Sciences, Beijing, 100085, China

ARTICLE INFO

Keywords:
Aging
EC
scRNA-seq

ABSTRACT

Aging is the strongest risk factor for cardiovascular disease, with progressive decline in the function of vascular endothelial cells (ECs) with age. Systematic analyses of the effects of aging on different cardiac EC types remain limited. Here, we constructed a scRNA atlas of EC transcriptomes in young and old mouse hearts. We identified 10 EC subclusters. The multidimensionally differential genes (DEGs) analysis across different EC clusters shows molecular changes with aging, showing the increase in the overall inflammatory microenvironment and the decrease in angiogenesis and cytoskeletal support capacity of aged ECs. And we performed an in-depth analysis of 3 special ECs, Immunology, Proliferating and Angiogenic. The Immunology EC seems highly associated with some immune regulatory functions, which decline with aging at different degrees. Analysis of two types of neovascular ECs, Proliferating, Angiogenic, implied that Angiogenic ECs can differentiate into multiple EC directions after initially originating from proliferating ECs. And aging leads to a decrease in the ability of vascular angiogenesis and differentiation. Finally, we summarized the effects of aging on cell signaling communication between different EC clusters. This cardiac EC atlas offers comprehensive insights into the molecular regulations of cardiovascular aging, and provides new directions for the prevention and treatment of age-related cardiovascular disease.

1. Introduction

Aging is the greatest risk factor that increases the incidence of cardiovascular disease. It can significantly alter heart structure and function, leading to biological processes associated with aging features, such as reduced autophagy, increased mitochondrial oxidative stress, telomere depletion, altered insulin-like growth factor signaling and growth differentiation activator and protein kinase pathways [1]. These conditions also occur frequently in the cardiac vascular system. Age-related cardiovascular changes are an important

* Corresponding author. State Key Laboratory of Ophthalmology, Zhongshan Ophthalmic Center, Sun Yat-sen University, Guangdong Provincial Key Laboratory of Ophthalmology and Visual Science, Guangzhou, 510060, China.
** Corresponding author.
E-mail addresses: zhangping@gzzoc.com (P. Zhang), zhyfeng@mail.sysu.edu.cn (Y. Zheng).
[1] Zhong Liu and Yanjing Huang have contributed equally.

https://doi.org/10.1016/j.heliyon.2023.e18324
Received 24 January 2023; Received in revised form 12 July 2023; Accepted 13 July 2023
Available online 22 July 2023
2405-8440/© 2023 The Authors. Published by Elsevier Ltd. This is an open access article under the CC BY-NC-ND license (http://creativecommons.org/licenses/by-nc-nd/4.0/).

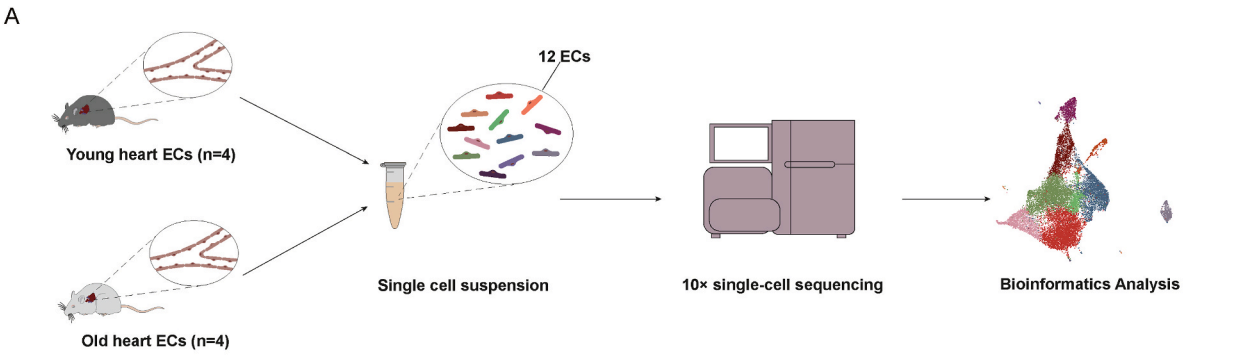

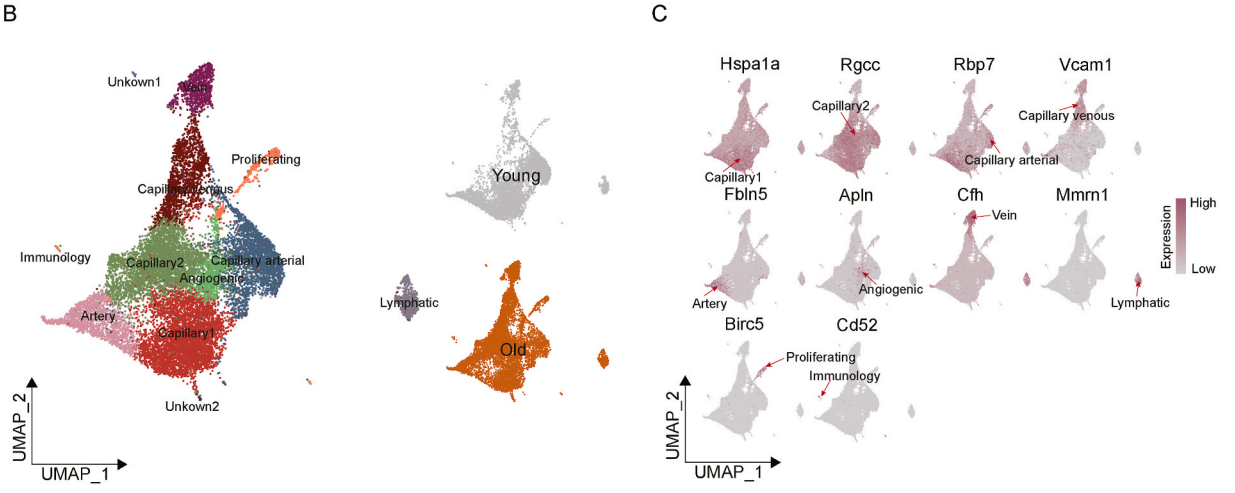

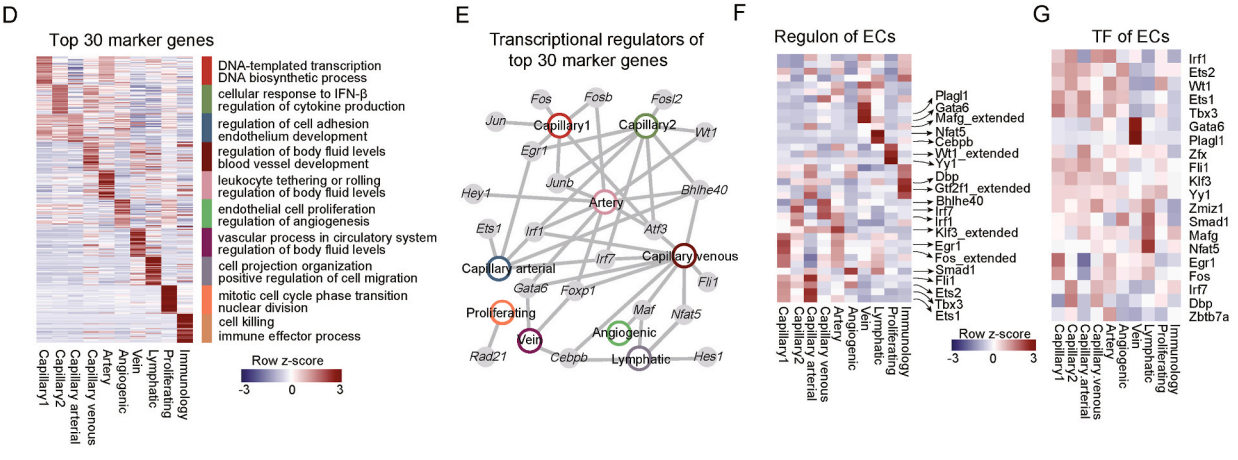

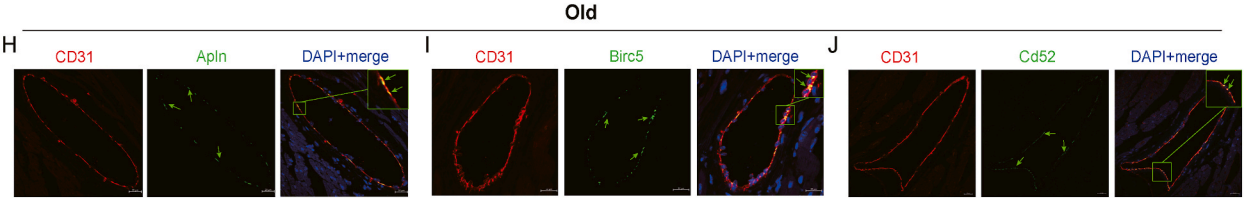

(caption on next page)

Fig. 1. Construction of single-cell sequencing atlas of mouse heart ECs. (A) Flow chart of scRNA-seq and bioinformatics analysis of Young and Old heart ECs. Young (female), n = 10630; Old (female), n = 6695. (B) Left panel: UMAP plots shows the different cell types and corresponding distribution of mouse heart ECs. Right panel. Distribution of ECs in the UMAP plots of Young and Old mouse. (C) Feature map shows the expression of cell type-specific marker genes in different clusters of mouse heart ECs. (D) Heat map shows the top 30 marker genes for specific clusters in the Old group with the enriched functional annotation of each marker gene on the right. (E) Network diagram shows the transcriptional regulators of the top 30 cluster-specific marker genes in all heart ECs. (F) Heat map shows specific regulators in different clusters of mouse heart ECs. (G) Heat map shows specific Transcription factor (TF) in different clusters of mouse heart ECs. (H–J) Representative micrographs of Old mouse heart sections, stained for an EC marker (CD31) and Apln (Angiogenic, H), Birc5 (Proliferating, I), Cd52 (Immunology, J) and counterstained with DAPI.

cause of cardiovascular diseases such as atherosclerosis [2,3]. The relationship between the endothelium and disease caused by aging has been investigated in more detail by other studies [4–6]. However, despite these efforts, the specific impacts of aging on different types of cardiovascular ECs remain less deeply explored. While some mechanisms have been described in greater detail than others, a more complete understanding of vascular ECs aging is important to develop measures to delay vascular aging and prevent the development of various cardiovascular diseases. For example, previous research has demonstrated that aging-related molecular changes occur in multiple cardiac cell types, including endothelial cells [7], which exhibit high mutations and instability in their genome [8].

Here, we describe a transcriptional atlas of single-cell RNA sequencing (scRNA-seq) in young and old mouse hearts, providing a comprehensive picture of the changes in the cellular and molecular complexity of aging at single-cell resolution. From this atlas, early dysregulated transcriptional changes in ECs can be visually identified. We analyzed the gene expression of multiple endothelial subsets and examined their potential biological functions. Specifically, we investigated the effects of aging factors on their gene expression and depicted some of the unique biological processes that arise in the aging vascular endothelium. Overall, our research improves the understanding of the aging process in cardiac ECs and provides a resource for potential therapeutic targets for aging-related cardiovascular diseases.

2. Results

2.1. Construction of single-cells transcriptomic atlas in ECs

To investigate the molecular characteristics of the aging heart endothelium, we captured each type of EC from different parts of the heart in different mouse. ECs from each sample were subjected to scRNA-seq by a 10x genomics-based protocol (Fig. 1A). We selected EC clusters as previous study [9] based on the expression of EC markers (Pecam1) and excluded pericytes (Pdgfrb), immune cells (Ptprc), smooth muscle cells (Acta2), fibroblasts (Col1a1) and erythrocytes (Hba-a1, Hba-a2, Hbb-bs). After rigorous quality control of the gene expression profile and filtering, a total of 17,325 eligible ECs from 4 young and 4 old mouse heart samples were retained and used for downstream analysis. Due to the effects of senescence on the vascular endothelium, we observed age-related differences in cell types and cell numbers (Fig. S1E). A total of 10 cell types were identified by the Uniform Manifold and Projection (UMAP) algorithm based on their unique gene expression characteristics (Fig. 1B). And the quality of cell sequencing of these types ECs basically meets the requirements of analysis (Figs. S1A–1D). The possibility of low mass and dead cells is basically excluded. Among these, some heart ECs types identified in both groups were previously characterized [9], and they included Capillary1(Hspa1a), Capillary2 (Rgcc), Capillary arterial (Rbp7), Capillary venous (Vcam1), Artery (Fbln5), Angiogenic (Apln), Vein (Cfh), Lymphatic (Mmrn1) ECs (Fig. 1C and Fig. S1F). Not only that, but we also identified other 2 special types of EC clusters, Immunology and Proliferating. And there were 2 unknow clusters. The Immunology ECs (Cd52) expressed multiple immune-related biomarkers and a variety of immunoglobulin-related genes and complement-related genes (Table S1). We found the coexistence of two ECs, Proliferating (Birc5/Top2a) and Angiogenic, with vascular EC regeneration ability in cardiac samples.

Then, we compared our own dataset with another aging mouse heart scRNA dataset [8] to observe the effect of various time points and different enrichment methods on the cell frequency of different cell clusters. The results showed that there were significant difference in the endothelial subpopulations of different age groups and different enrichment methods (Fig. S1E and Table S7). The endothelial frequency was further altered when the batch effect was removed after the integration analysis, suggesting a large influence of the batch effect (Fig. S1E). Therefore, considering the batch effect from different sequencing technologies and enrichment methods, the subsequent analysis still used our original data.

For each of the cell type, we identified a set of Top50 markers (Table S1). Gene Ontology (GO) analysis of the Top30 marker genes demonstrated functional characteristics of the corresponding cell type (Fig. 1D). For example, “DNA synthesis and transcriptional processes” was enriched for Capillary1, which was predominant in the young mice. On the other hand, “regulation of cytokines production and cellular response to IFN-β” was enriched for Capillary2, the predominant in the old mice. In addition, “body fluid balance regulation” was enriched for ECs associated with either Artery or Vein (Artery, Vein, Capillary venous), “Signal reception and cell killing processes” for the Immunology ECs, “Regulation of endothelial proliferation and sprouting” for the Proliferating ECs, and “cell cycle transition and further mitotic proliferation” for the Angiogenic ECs.

We also investigated the molecular mechanisms driving EC phenotypic differentiation using single-cell regulatory network inference and clustering (SCENIC). We compiled a regulatory network of transcription factors (TFs) of Top30 marker genes, defining key TFs for each ECs and TFs cross different cell types (Fig. 1E). These transcription factors determine the phenotypic characteristics of ECs. In addition to this, we analyzed the regulons that have the greatest impact on each type of ECs (Fig. 1F), clarifying the regulation strength of each regulon for different cell types. We also showed the expression of transcription factors corresponding to these

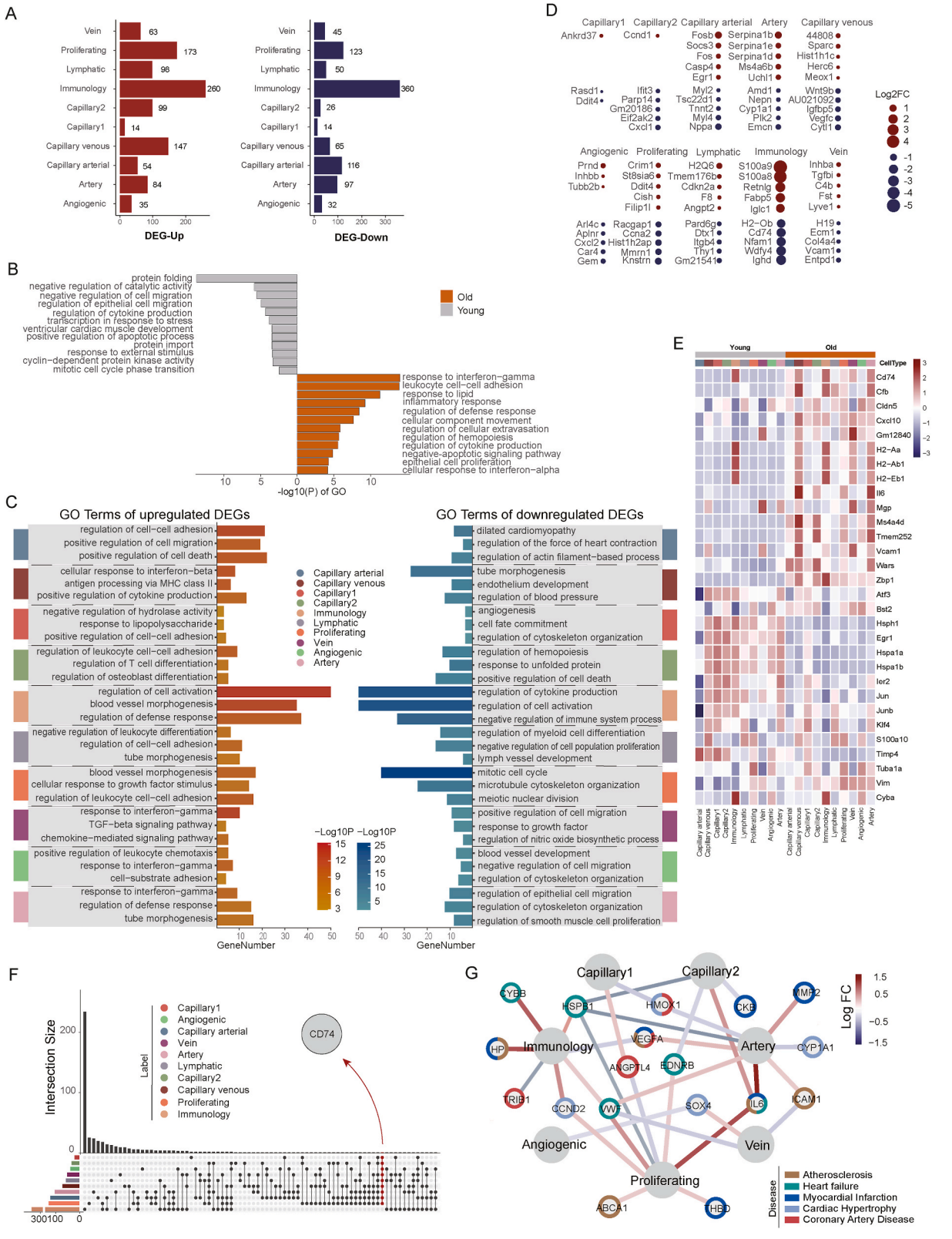

(caption on next page)

Fig. 2. Multidimensional molecular characteristics of aging mouse heart ECs (A) Histogram plot shows aging-associated up- and down-regulated differentially expressed genes (DEGs) (adjusted *P*-value <0.05, |LogFC| > 0.25). (B) Bar graph shows the GO terms for overall DEGs between the Young and Old groups. (C) Graph shows significant GO terms or pathways for DEGs in 10 cell types in mouse heart ECs. (D) Dot plots shows the top five cell type-specific DEGs for all clusters. Up-regulated genes are shown in red, while down-regulated genes are shown in blue. (E) Heat map shows the gene expression of DEGs that are simultaneously expressed in at least three clusters in different EC clusters. (F) Graph shows the number of specific up-regulated DEGs in each cluster and the intersecting DEGs in different clusters. CD74, which expressed in the most clusters are marked. (G) Network diagram shows DEGs associated with cardiovascular disease in different cell types of mouse heart ECs. (For interpretation of the references to color in this figure legend, the reader is referred to the Web version of this article.)

regulators (Fig. 1G).

The double immunostaining of IF and FISH for an EC marker (CD31) and the markers of these specialized EC phenotypes confirmed the scRNA-seq data (Fig. 1H–J; Figs. S1G–S1I).

2.2. Characterization of aging-related molecular features in ECs

In order to further identify the effect of aging on cardiovascular endothelium molecular function, we analyzed the overall differentially expressed genes (DEGs) in the young and old heart ECs (Fig. 2A and Table S2). We found that "protein folding" was enriched for downregulated DEGs in early stage; whereas increased expression of genes involved in "IFN responses", "rolling adhesion of leukocytes" and "immune responses" suggested the potential for increased inflammatory signatures in the micro-environment in later stages of aging (Fig. 2B). These observations are consistent with previous research on aging heart [7,10]. Next, to dissect cell type-specific changes in gene expression, we identified key cell types and molecular mechanisms affected by cardiac senescence by showing various age-related DEGs that were differentially expressed in at least one cell type in old versus young hearts (Table S2). We found that the highest numbers of DEGs occurred in the Immunology, Proliferating, and Capillary venous regions (360, 123, and 65 up-regulated genes, and 260, 173, and 147 down-regulated genes, respectively, in the aged hearts) (Fig. 2A). Apart from this, the proportions of these cells also differed significantly between the young and old hearts (Fig. S1E), suggesting that these may be the cell types more strongly affected by aging.

Next, we investigated the molecular pathways most affected by aging in these cell types through functional annotation enrichment analysis. We noted that "regulation to heart function, blood pressure, and myofilament functions" were enriched in the down-regulated DEGs in the Capillary arterial and Capillary venous ECs (Fig. 2C), suggesting that genes associated with microvascular contraction and cardiac regulation were dysregulated in an early transcriptional stage. "regulation of cytoskeleton organization" were also enriched in the down-regulated DEGs in the Capillary1, Proliferating, Angiogenic and Artery ECs (Fig. 2C), implying for a correlation between impaired cellular support and aging [11]. In addition, age-related upregulated DEGs in Capillary arterial, Capillary1, Capillary2, Lymphatic, Proliferating and Vein ECs were enriched in "cell adhesion", pointing to a link between cell adhesion and EC aging [12]. Furthermore, "Cell cycle transition and nuclear division", "angiogenesis", and "vascular and endothelial development" were enriched in down-regulated DEGs in Proliferating-, Capillary1-, Angiogenic- and Capillary venous-ECs, respectively, suggesting the impairment of neovascular function by aging, which is consistent with previous findings [13,14]. Finally, almost all types of aging-related upregulated DEGs in ECs were associated with "inflammation" and "Immune-related process" (Fig. 2C), pointing to that the correlation between aging and inflammation is universal across different ECs [4,15].

To further investigate the impacts of aging on different EC subtypes, we examined cell-type-specific DEGs and identified the top 5 genes for each cell type (Fig. 2D). These dysregulated genes may underlie the progressive endothelial decline in the heart during aging. Among these, the rs6647 variant G allele in Serpina1 family genes, which was upregulated in aged Artery ECs, has been reported to be associated with the risk of large-artery atherosclerotic stroke (LAS) (Fig. 2D) [16]. We also found that S100a8/a9 was upregulated in aged Immunology EC (Fig. 2D). Previous studies have identified the link between S100a8/a9 and mitochondrial dysfunction as well as cardiomyocyte death in response to ischemia-reperfusion injury [17]. Intriguingly, S100a8/a9 has also been reported to be an inflammatory marker that determines the prognosis of COVID-19 [18]. And further studies could be explored to investigate the role of S100a8/a9 during COVID-19 infection and mortality among elderly patients.

We also identified the Top15 up- and down-regulated genes that affected the majority of ECs types (Fig. 2E). The results showed that inflammation-related genes CD74 and Cxcl10 were expressed in 9 EC types (Fig. 2E) and they were the most significantly upregulated genes in aged hearts (Table S2) [19,20]. We also noted upregulated histones H2Aa, H2Ab1, and H2Eb1, all of them showing highly consistent expression trends. They may have synergistic effect on aging process [21,22]. In addition, we identified the increased expression of Vcam1 gene in many ECs (Fig. 2E), supporting a correlation between vascular cell adhesion and cardiac aging [12,23]. Finally, we listed 80 intersections of the same DEGs in these cell populations, which allow us to identify which EC cell types are similarly affected by aging (Fig. 2F and Fig. S1L).

To annotate hotspot genes associated with age-related diseases in ECs, we performed a comprehensive comparative analysis between age-related DEGs and cardiovascular disease annotated genes from the Aging Atlas gene set (Fig. 2G). We found that the Immunology, Proliferating and Artery ECs are rich in most high-risk DEGs, suggesting that these three cell types may be more susceptible to age-related cardiovascular disease. Of these, Heat Shock Protein Family B Member 1 (HSPB1) and Von Willebrand Factor (VWF) were both expressed in all the three cell types, which were associated with heart failure (Fig. 2G). Homologous oxidized HSPB1 (homo-oxidized HSPB1) attenuates oxidative stress injury in cardiomyocytes [24], and its specific knockout exacerbates cardiac dysfunction through NFkB-mediated leukocyte recruitment [25]. In contrast, VWF exists as an indicator of endothelial dysfunction due to prolonged heart failure [26]. We also identified some high-risk DEGs that are associated with multiple diseases (Fig. 2G). For

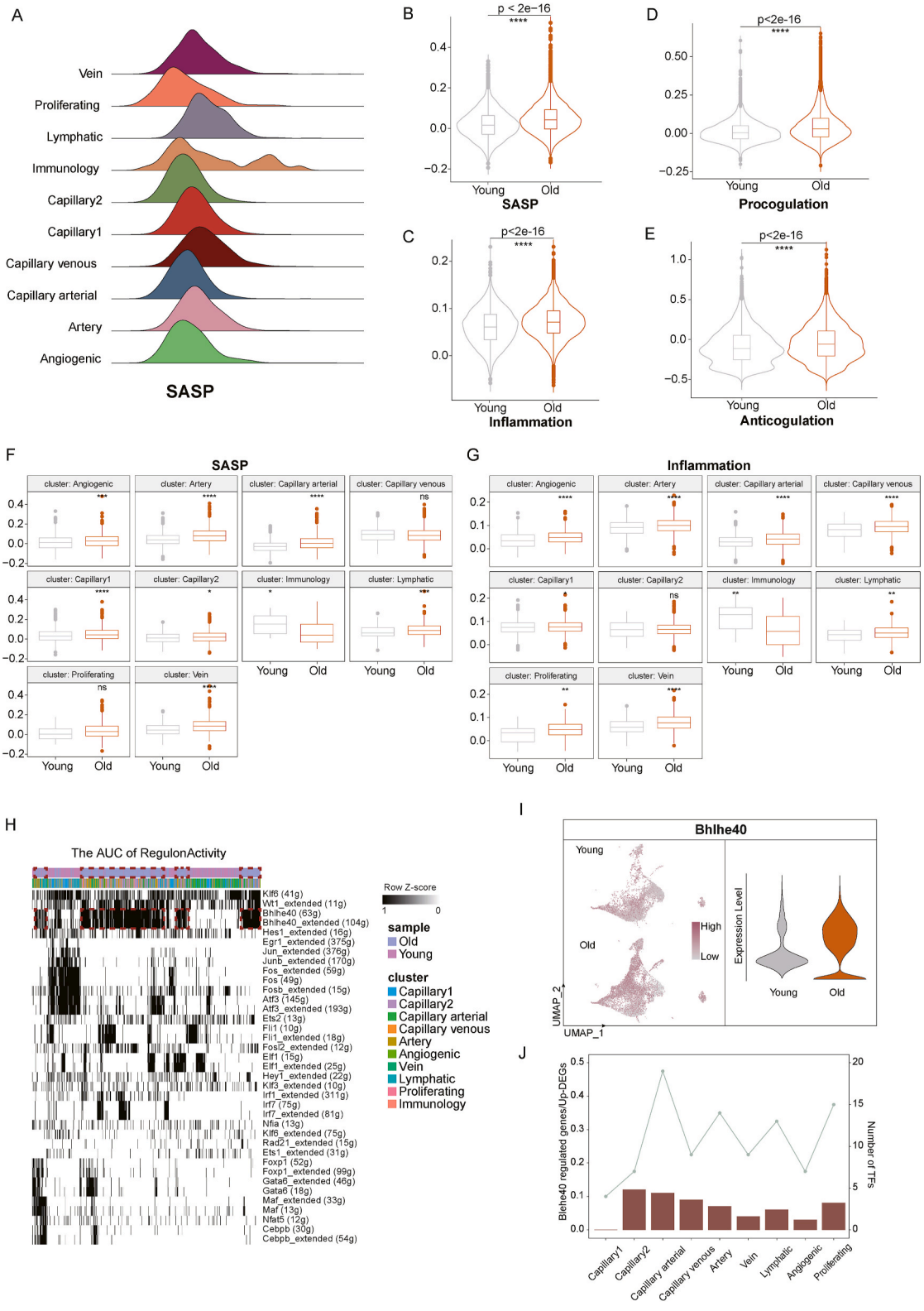

Fig. 3. Analysis of mouse heart endothelial aging phenotypes and drivers. (A) Ridge plots shows gene set scores associated with SASP gene set. (B–C) Violin plot shows changes in SASP(B) and Inflammation(C) gene set scores with age in all ECs of Young and Old mouse hearts. (D–E) Violin plot shows changes in Procogulation(D) and Anticogulation(E) gene set scores with age in all ECs of Young and Old mouse hearts. (F–G) Boxplot shows changes in SASP(F) and Inflammation(G) gene set scores with age in different EC clusters. (H) Heat map shows regulator activity scored by

the AUC method, Bhlhe40 is highlighted as it is closely associated with the aging group. (I) Feature plot and violin plot shows the expression of Bhlhe40 gene in Young and Old mouse heart ECs. (J) The upper line plot shows the number of TFs in each cluster and the lower bars represent the proportion of Bhlhe40-regulated and upregulated differentially expressed genes in Old mouse heart ECs.

example, Vascular endothelial growth factor A (VEGFA) has been shown to be associated with inflammatory environmental stimuli in the aged heart and various cardiovascular diseases [27]. IL-6 has also been shown to be associated with atherosclerosis, heart failure, and myocardial Infarction (Fig. 2G) [28].

Taken together, we have characterized the aging-related molecular profile of the cardiac endothelium, suggesting that the impaired cytoskeletal vascular neovascularization and increased cellular adhesion and inflammatory responses may be the most affected functional features of age-related endothelial degeneration in the heart.

2.3. Profiling of phenotypes and potential drivers of aging in ECs

2.3.1. Aging phenotypic related analyses

Senescence-associated secretory phenotype (SASP) genes are traditionally considered as aging-related biomarkers [29] (Table S4). Thus, we compared the SASP scores of different ECs. We found that SASP scores were relatively low in Angiogenic and Proliferative ECs (Fig. 3A). We also compared the scores of inflammatory gene set. Consistent with other tissues, the inflammatory score and SASP score of EC were significantly higher in the old hearts than in the young ones (Fig. 3B and C) [30]. Besides, we also compared the differences of SASP and Inflammation scores in the same EC cell type between young and old hearts. We found that many ECs clusters (except for Capillary venous, Immunology and Proliferating ECs) had a higher SASP score in the old hearts (Fig. 3F), and except for Capillary2, Immunology ECs, basically all aging endothelial clusters exhibit higher levels of inflammation score (Fig. 3G). In general, these two results are in good agreement. It is worth noting, however, that the Immunology EC scored higher in the young mouse for SASP and

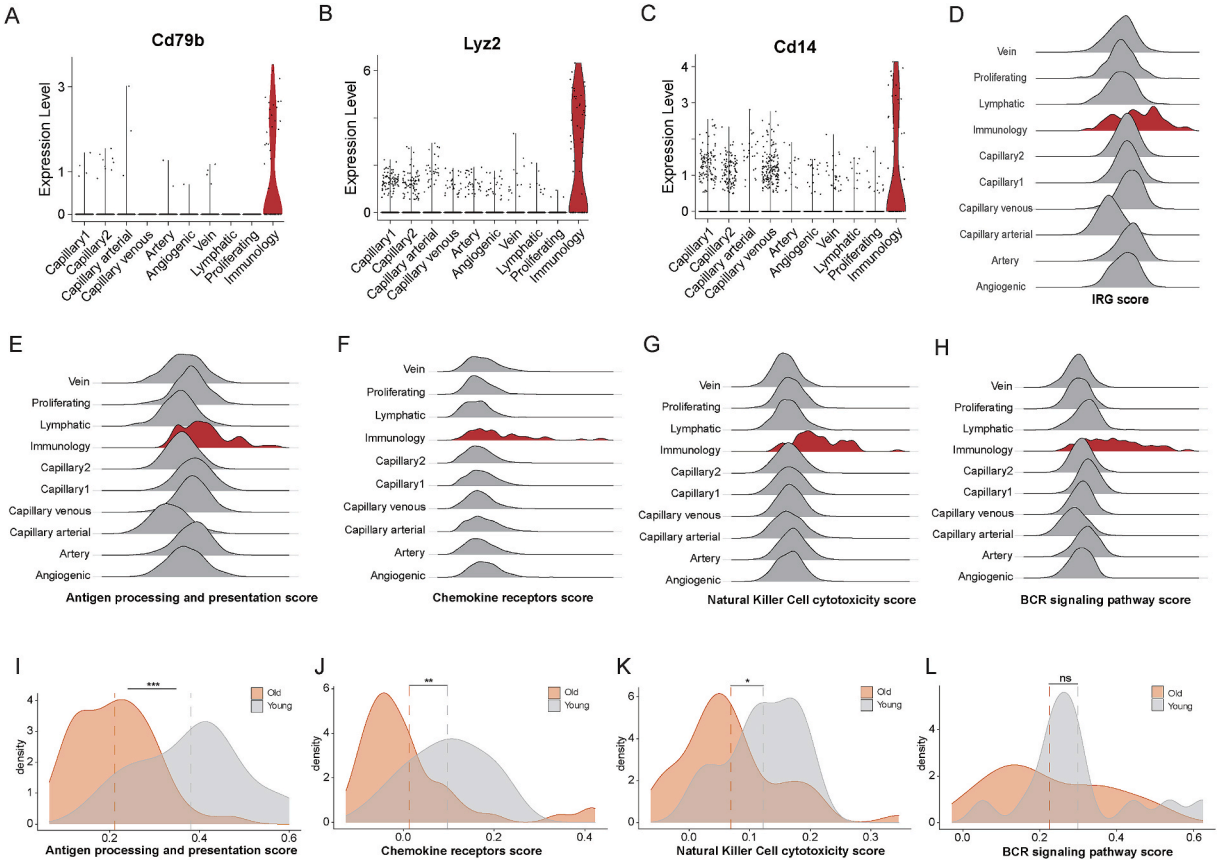

Fig. 4. Analysis of Immunology EC for mouse hearts. (A–C) Violin plot shows the expression of the genes Cd79b(A), Lyz2(B), Cd14(C) in each EC cluster. (D) Ridge plots showing gene set scores associated with IRG set. (E–H) Ridge plots showing gene set scores associated with Antigen processing and presentation(E), Chemokine receptors(F), Natural Killer Cell cytotoxicity(G), BCR signaling pathway(H) gene set. (I–L) Density plot shows the Antigen processing and presentation(I), Chemokine receptors(J), Natural Killer Cell cytotoxicity(K), BCR signaling pathway(L) gene set score of the Immunology EC for Young and Old hearts. The dotted line represents the mean score. ns $P > 0.05$, *$P < 0.05$, **$P < 0.01$, ***$P < 0.001$, ****$P < 0.0001$.

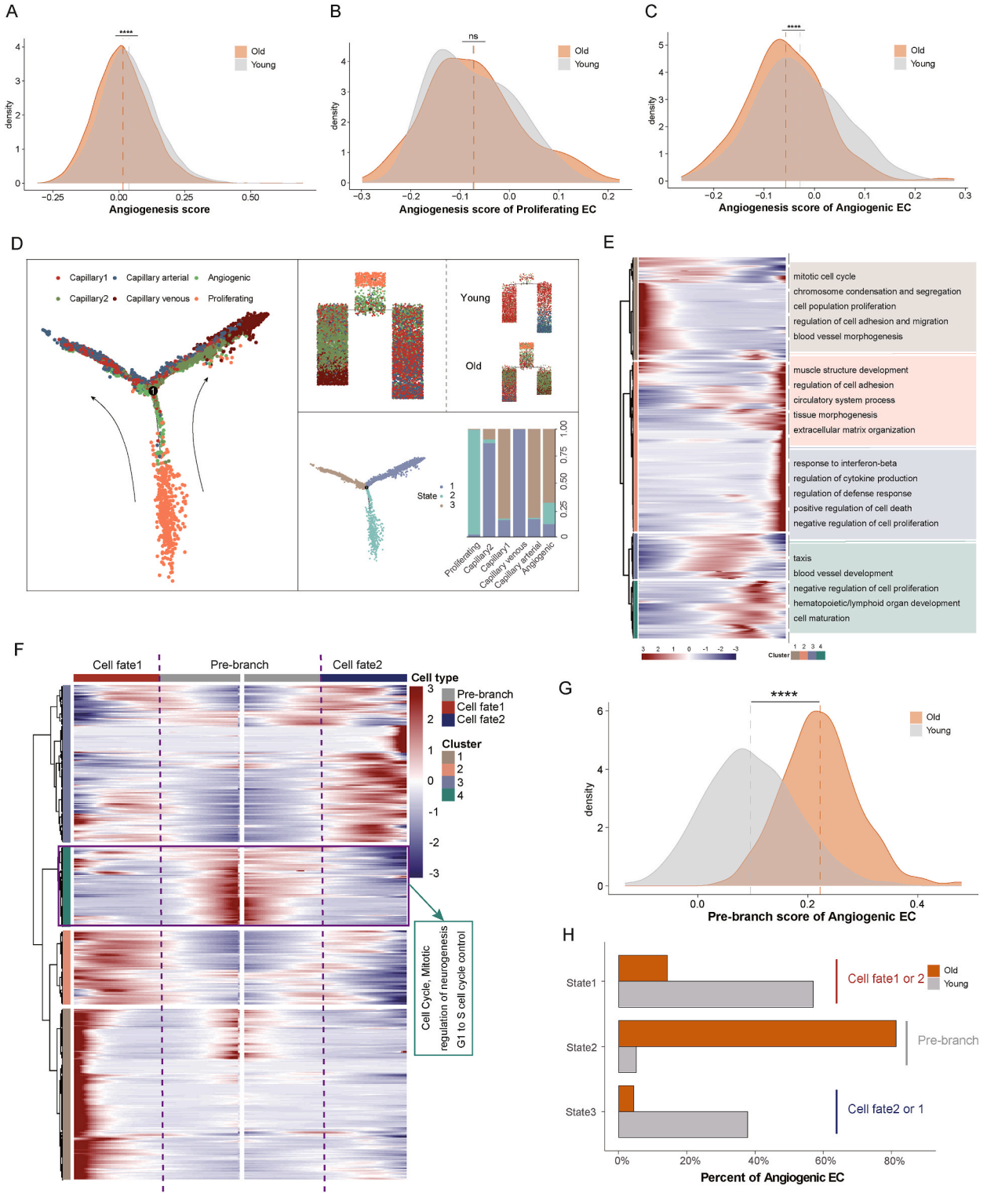

(caption on next page)

Fig. 5. Analysis of neovascular endothelium, Proliferating and Angiogenic EC for mouse hearts. (A) Density plot shows the Angiogenesis gene set score of overall ECs for Young and Old hearts. The dotted line represents the mean score. ns $P > 0.05$, *$P < 0.05$, **$P < 0.01$, ***$P < 0.001$, ****$P < 0.0001$. (B–C) Density plot shows the Angiogenesis gene set score of Proliferating EC(B), Angiogenic EC(C) for Young and Old hearts. The dotted line represents the mean score. ns $P > 0.05$, *$P < 0.05$, **$P < 0.01$, ***$P < 0.001$, ****$P < 0.0001$. (D) Pseudo-time analysis of six specific cell types (Capillary 1, Capillary 2, Capillary artery, Capillary venous, Angiogenic, Proliferating) in heart ECs (Young and Old integrated). The tree plot shows the differentiation trajectories of the integrated heart EC samples and the differentiation trajectories of Young and Old heart ECs, respectively. The state analysis and histogram show the proportions of the three states in each EC cluster. (E) Heat map shows the expression profiles of all genes in the trajectory along the pseudo-time, divided into four clusters, whose GO enrichment analysis is on the right. (F) Heat map shows the alignment of genes in branch node 1 and divided into four clusters. (G) Density plot shows the pre-branch state score of Angiogenic EC for Young and Old hearts. The dotted line represents the mean score. ns $P > 0.05$, *$P < 0.05$, **$P < 0.01$, ***$P < 0.001$, ****$P < 0.0001$. (H) The histogram shows the proportion of Young and Old Angiogenic EC in the three types of sates. State2 can be understood as the pre-branch state.

Inflammation gene sets. We speculate that this result may be due to a more active immune state in the Immunology EC of the young hearts. Regardless, the differences in SASP and Inflammation score in various ECs also reflect their heterogeneity in aging extent.

In addition, we also examined the overall coagulation function of ECs of the aging and young mouse. Similar to previous report of other tissues, senescent endothelial cells exhibited higher levels of anticoagulant and procoagulant states (Fig. 3D and E) [30]. These results may represent a disordered clotting state in the endothelium of the heart of aging mice and certain pathological states of aging.

2.3.2. Transcriptional regulatory analyses

Based on the binary heat map results, we observed that the Bhlhe40 regulon exerted a regulatory effect on almost all ECs in old hearts (Fig. 3H), whereas this was rarely the case for the ECs in young hearts. Thus, Bhlhe40 may be one of the drivers of the EC senescence process. We compared the distribution of Bhlhe40 expression in young and old hearts (Fig. 3I). Furthermore, to assess the contribution of Bhlhe40 to each class of EC type in aging hearts, we analyzed the percentage of aging-upregulated DEGs regulated by Bhlhe40 in the total aging-upregulated DEGs (Fig. 3J). Finally, to evaluate the degree of regulation specificity of Bhlhe40 for each aging ECs, we present the total number of transcription factors for the upregulated DEGs/Top 50 marker genes using a line graph format (Fig. 3J).

2.3.3. Aging impairs the immune regulatory function of immunology EC

Next, we conduct a detailed analysis of Immunology EC. We found the Immunology EC expressed specifically multiple immune-related biomarkers, such as the Cd79b (B cell) (Fig. 4A) [31], Lyz2 (Macrophages) (Fig. 4B) [32], Cd14 (Fig. 4C) (Monocyte) [33]. Since immune cells (Cd45/Ptprc) have been excluded, we believe that this is a type of EC that is highly associated with immune function. To further confirm our hypothesis, we scored the immune-related gene (IRG) gene set for all ECs, and found that this EC does have a greater correlation with IRG (Fig. 4D) [34].To further explore the specific immune regulatory functions of this EC, we scored a number of different functions summarized by the IRG gene set separately. The results showed that the Immunology EC exhibited significantly higher scores in “antigen processing and presentation”, “chemokine receptors”, “natural killer cell cytotoxicity” and “natural killer cell cytotoxicity” (Fig. 4E–H, S2A-S2I), which may reflect that the Immunology EC plays a significant role in these immunomodulatory functions.

After that, we compared the immunomodulatory capacity of Immunology EC between the young and old groups, respectively. The results showed that significant differences of gene set scores in “antigen processing and presentation”, “secrete Chemokine receptors”, “and exert the ability of Natural Killer Cell cytotoxicity” (Fig. 4I–K). Although the involvement of this EC in the BCR signaling pathway process can also be reduced, this effect is not significant enough (Fig. 4L). These results are consistent with the above-mentioned decrease in the expression of inflammatory factors in the aging Immunology EC compared to the younger (Fig. 3G), which may reflect a decrease in immune-related function with aging [35,36].

In summary, we identified a class of ECs involved in immune regulation. And our findings suggested that aging may lead to a decline in a variety of immune regulatory abilities.

Aging impairs the angiogenesis and differentiation ability of neovascular ECs without changing the direction of differentiation of endothelial lineages.

We conducted an in-depth analysis of Proliferating, Angiogenic EC to explore the effects of aging on vascular endothelial growth and development. Consistent with previous studies [14], we have observed that there is a significant decrease of angiogenesis score in senescent endothelium overall (Fig. 5A). Our discoveries of two types of angiogenesis-related ECs, Proliferating and Angiogenic, aided in our studies of how aging affects these cells. Our results showed that senescent Angiogenic EC exhibited a significant decrease in angiogenesis capacity (Fig. 5C), whereas Proliferating EC did not (Fig. 5B). These findings may point to the potential mechanism of the decline in angiogenesis with aging.

Next, we explore whether aging also change the differentiation directions of the neovascular ECs. It has been shown that nascent vasculature has the ability to differentiate in different directions in Venous, Arterial [37], but whether the differentiation trajectory changes with age remains unclear. To investigate whether the differentiation trajectory and molecular changes in neovascular ECs occur with age, we subjected Capillary, Capillary venous, Capillary arterial, Proliferating, and Angiogenic EC cells to pseudo-temporal analysis. We observed that Capillary2 and Capillary venous are essentially in state1, while most of the cells in Capillary1 and Capillary arterial are in state3, which implies similarities in the states of differentiation between them (Fig. 5D). In addition, Proliferating is in the state2 of initiation of differentiation, while Angiogenic is evenly distributed across the three cellular states (Fig. 5D). These results showed a progressive differentiation from Proliferating ECs (as the starting point), to Angiogenic ECs and finally to the state in which

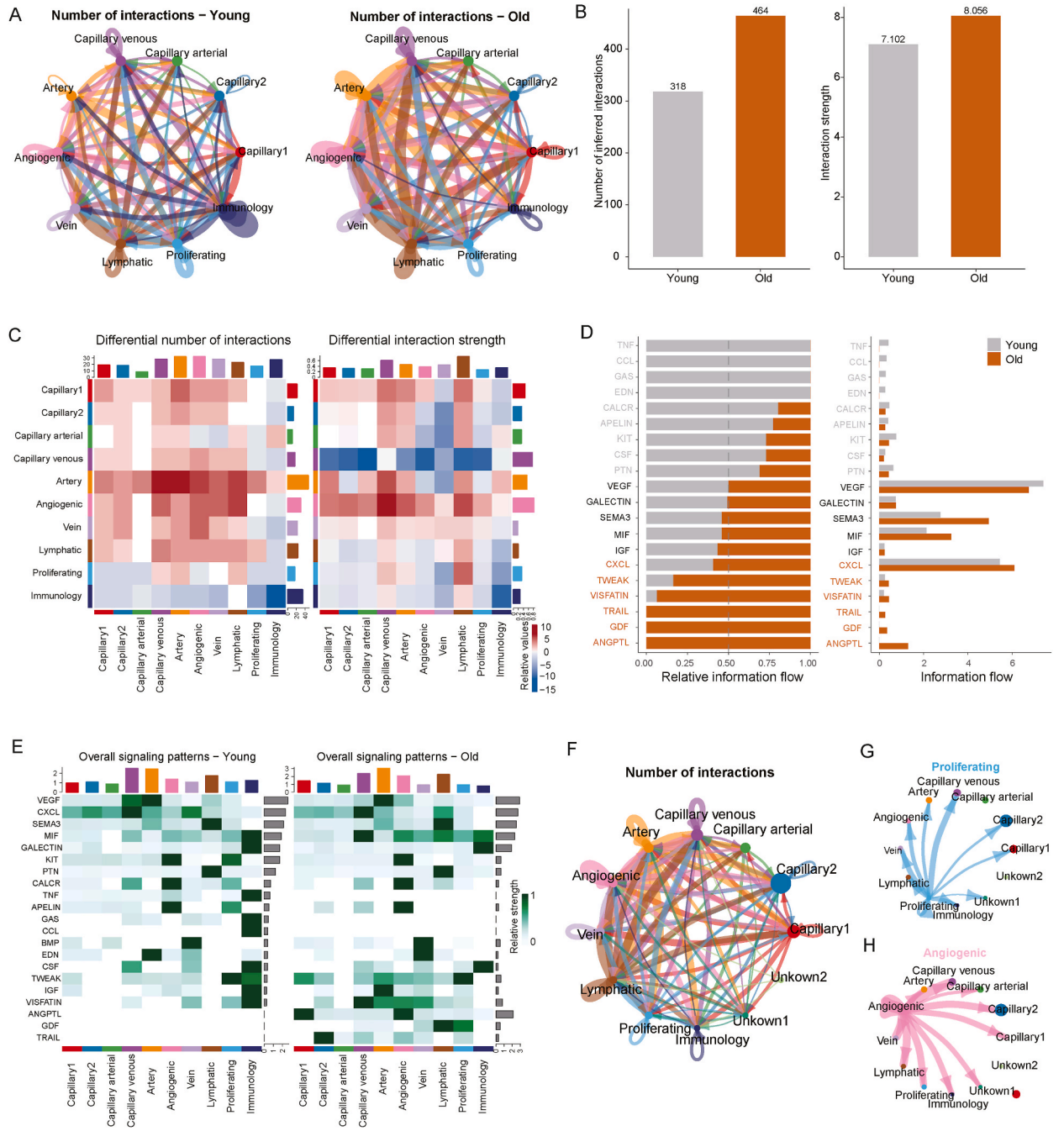

Fig. 6. Analysis of the effects of aging on endothelial signaling communication. (A) Circular network diagram shows the number of cell-cell interaction in Young and Old hearts sample, with arrows and edge colors indicating the pathway direction (ligand-receptor). The edge thickness indicates the sum of the number of interpopulation interactions. (B) Histogram counts the number and interaction strength of cell-to-cell interactions in Young and Old heart samples. (C) Heat map shows the difference in cell-cell interactions of various EC clusters between the Young and Old heart samples. The plot on the left is based on the number of interactions and the plot on the right is based on the weights. Red color represents up-regulation of interactions compared to the Young group and blue color represents down-regulation of interactions. (D) Bar graph shows predicted pathways for Young and Old heart ECs, with gray labels representing pathways in the Young group, black representing pathways shared by the Young and Old groups, and orange representing pathways in the Old group. (E) Heat map showing comparison of overall different signaling pathway intensities between Young and Old heart ECs. The relative intensity is colored in a gradient from white to green. (F) Circular network diagram shows the number of cell-cell interaction in Old hearts sample, with arrows and edge colors indicating the pathway direction (ligand-receptor). The edge thickness indicates the sum of the number of interpopulation interactions. (G–H) Circular network diagram shows the cellular communication paradigm when the Proliferating(G), Angiogenic(H) EC as the signaler. (For interpretation of the references to color in this figure legend, the reader is referred to the Web version of this article.)

different ECs of Capillary1, Capillary2, Capillary venous and Capillary arterial are located. This result suggests that the Proliferating EC may act as the "initiator" of the new EC sprouting, while the Angiogenic EC is more like the "executor" of the differentiation into various ECs. This is in agreement with the overall temporal trend in the UMAP diagram (Fig. S3A). The direction of differentiation trajectory is consistent with the separate data from the young and old hearts ECs in tree plot (Fig. 5D), and is also consistent with previous findings [37]. In addition, we established a potential molecular cascade along the pseudo-temporal trajectory. We found that the proliferating marker gene Birc5 was located at the beginning of the trajectory and was expressed at a decreasing level during differentiation (Fig. S3F). In addition, the marker genes expression trends for Capillary1, Capillary2, Capillary venous, Capillary arterial, and Angiogenic EC, were in agreement with their respective positions on the time trajectories (Figure S3B-S3E and Figure S3G), verifying the credibility of time trajectories. These results suggested that aging may not alter the general direction of nascent blood vessels differentiation.

We further explore whether aging impairs the differentiation ability of neovascular ECs. The stage-specific gene expression along pseudo-time was clustered to obtain four distinct clusters of gene expression profiles, and we analyzed their corresponding enriched GO terms (Fig. 5E and Table S6). Custer 1 genes enriched in functions regulating "cell proliferation and nuclear division", "early vascular morphogenesis" and "chromatin regulation" were progressively down-regulated over time (Fig. 5E). In contrast, the genes defined by cluster 2 were progressively up-regulated along the trajectory and characterize genes involved in the "circulatory processes" and "cell adhesion" processes of the mature endothelium (Fig. 5E). These results prove that there is a chronological relationship between these ECs' genes. We then proceeded to analyze branch point 1 genes in neovascular EC differentiation, aiming to identify key genes that promote differentiation. Clustering of branchpoint-specific gene expression along pseudo-times yielded four distinct clusters. We found that cluster 4 seemed to be more closely associated with pre-branch status (Fig. 5F and Table S6) , which can be understood as undifferentiated state2. We found that aging Angiogenic EC has a greater tendency to express the pre-branch state gene (Fig. 5G), and a larger proportion of its cells are in the pre-branch state (undifferentiated state) (Fig. 5H). These results mean that aging Angiogenic EC may have a harder time reaching mature states (1 and 3) and may not be able to perform differentiation functions well.

We further analyzed the mechanisms of the production of two neovascular ECs. We summarized all the signaling pathways acting on the two types of neovascular ECs and found that their signal pathways were very similar (Figure S3H and Figure S3I). The results show that capillary venous and Artery EC affected Proliferating and Angiogenic EC cells mainly through the multiple VEGF pathways, which is critically important for neovascularization (Figure S3H and Figure S3I) [38]. Tnfsf family of genes, which are associated with ischaemic vascular diseases [39], significantly regulated both Proliferating and Angiogenic biological processes (Figure S3H and Figure S3I). In addition, both ECs contain a large number of signaling pathways of the Sema3 family, which have previously been thought to be involved in pathological angiogenesis and remodeling processes (Figure S3H and Figure S3I) [40]. We also found that Kitl/Kit was a common pathway for all endothelial regulation of Angiogenic ECs (Fig. S3I), which was previously thought to regulate stem cell proliferation and differentiation behavior [41–43].

Considering the tendency that aging leads to a decrease in the ability of angiogenesis and lineage differentiation of Proliferating EC and Angiogenic EC, we analyzed the transcriptional regulatory network of aging-associated DEGs in the two cell types. We identified a set of key transcription factors regulating aging-associated DEGs, including Interferon Regulatory Factor 1 (IRF1), Basic Helix-Loop-Helix Family Member E40 (BHLHE40), Early Growth Response 1 (EGR1), jun B proto-oncogene (JUNB), Activating Transcription Factor 3 (ATF3), etc (Figure S3J and Figure S3K). In both groups of cells, we identified Egr1 that has been previously associated with VEGFR signaling and angiogenesis [44,45], and which regulates multiple down-regulated DEGs. Besides, Similarly, Junb has also been reported to have a pro-angiogenic function [46] and was found to regulate many down-regulated DEGs in our study. These results may have implications for future research to explain why the aging heart have a reduced capacity in angiogenesis.

Taken together, our analysis depicted the effects of aging on angiogenesis and differentiation in ECs, revealing the complete trajectory of cardiovascular endothelial, exploring potential mechanisms of angiogenesis and differentiation of ECs.

2.3.4. Profiling of the effects to ECs cellular communication and molecular signaling pathways of aging

To investigate endothelial cell-to-cell interactions between the young and old groups, we used Cellchat algorithm [47] to analyze ECs. The results showed that the signal communication intensity between the aging group was stronger (Fig. 6A and B), suggesting that the amount and intensity of endothelial cell-to-cell communication increases with age. We then explored the changes in the number and intensity of signaling between each EC clusters. The results showed that the number of signal effects was generally increased except for Proliferating and Immunology, and the intensity changes were different upon different ECs (Fig. 6C). These results supported that senescent ECs may fall into a state of stress where signals are overcommunicated. In addition, we compared the signaling pathways between the two groups, identified the signaling pathways unique to the young group and the old group (Fig. 6D), and evaluated the contribution of each endothelium in these unique pathways (Figs. S4A–S4G). Among them, the Immunology EC has made significant contributions to the young unique TNF, CCL, GAS signaling pathway (Figs. S4A–S4C), which pointed to that aging may lead to a decline of some immune-related pathways in Immunology EC. We then described all the overall signaling patterns between the two groups in the form of heat maps, and compared the strength of each EC participation in different signaling pathways between the two groups (Fig. 6E).

Next, we analyze the signal communication situation of the old ECs sample separately. We showed the number and strength of interactions between EC cells (Fig. 6F and Fig. S4H). Lymphatic ECs had more ligand receptor pathways in signaling communication with other ECs, suggesting a tight signaling association between aging lymphatic and vascular endothelium (Fig. 6F and Fig. S4P). The effects of Artery EC cells may be linked to the many histopathological changes in the heart following arterial senescence (Fig. 6F and Fig. S4L). In addition, the Proliferating and Angiogenic EC cells also exert signaling effects on other ECs (Fig. 6F, G and Fig. 6H). To visualize the interaction network, we arranged the signals for each EC type separately (Fig. 6G and H and Fig. S4I-P). To identify the

inner connection between the action modes of each signaling pathway, we sorted out communication patterns of each cell and corresponding pathways (Figure S4Q and Figure S4R).

Overall, our cellchat analysis depicted the relationships of cardiac vascular EC signaling interactions networks and reveals potential molecular signaling pathways changes with aging.

3. Discussion

So far, there have been some studies that utilize single-cell sequencing technology to analyze the effects of aging on heart tissue [8,9]. They focused on describing the overall changes in the parenchymal and interstitial cells of the heart caused by aging to explore the association between aging and cardiovascular system diseases. However, an important reason for the decline in cardiovascular system function due to aging is the weakening of the physiological function of the vascular endothelium. The heterogeneous effects of aging on different vascular endotheliums are still worth exploring. However, the single-cell data endothelial cells of previous aging hearts have not been enriched and captured [8,9], so it is difficult to depict a more complete map of aging endothelial subsets due to the lack of adequate amounts of ECs. In addition, the exact effects and mechanisms of aging on various vascular ECs have likewise not been determined.

Firstly, we constructed the first single-cell map of senescent cardiac ECs and identified 10 different types of ECs (Fig. 1B). Apart from these traditionally identified cell types [9], we also identified an immune-related EC and two EC classes specific to the senescent heart. We also used GO analysis to confirm the biological functions of various ECs.

Secondly, we performed a multidimensional analysis of the effects of aging on EC subsets. We investigated the heterogeneity of the extent to which the ECs is affected by aging and found that Immunology, Proliferating and Capillary venous are the cells most affected by aging, because they exhibited the majority of DEGs. Next, we analyzed the heterogeneity of the aging state of the ECs. There was damage to the cytoskeletal support of certain endothelial subpopulations, and a decrease in the ability of angiogenesis during the early transcription of cardiac aging. In addition, the endothelial microenvironment exhibits increased inflammation. These findings are in line with the results from previous reports (Fig. 2C) [4,11,13,14]. We also demonstrated the heterogeneity (Fig. 2D) and similarity effects (Fig. 2E and F and Fig. S1L) of aging on cells in various subpopulations through various methods. We substituted the DEGs into the human disease gene set to form an aging-related heart disease network. This allows us to identify the aging gene in EC that causes human cardiovascular disease (Fig. 2G).

Thirdly, we identified a subpopulation of Immunology EC in the endothelium of the heart. Our functional analysis revealed that it has a clear association with immunomodulation. In line with our findings, there have been several previous literature reports of EC immune functions. The researchers found that the endothelium can express major histocompatibility complex class II (MHC-II) surface molecule HLA-DR to present antigens and activate T cells [48–50]. Moreover, the endothelium is also capable of recruiting different immune cells simultaneously through various adhesion molecules, selectors, and pro-inflammatory factors [51–54]In addition, several studies have demonstrated that organ-specific endothelial immune regulatory behaviors exist, including lymph nodes, livers, lungs, kidneys, brains, etc [55–62].

In this study, we found that such cardiac ECs can specifically express immune-related genes and discovered its various immunomodulatory functions. In addition, we found that aging weakens many immune-regulating abilities to varying degrees. Consistent with our conclusions, previous reports have shown that aging indeed can have a huge impact on the physiological function of immune-related cells. For example, the ability of aging naïve Treg CD4 T cells to form high-function immune synapses is reduced, resulting in naïve CD4 T cells being unable to produce cytokines and differentiate to exert immune function [63,64]. The ability of CD8 T cells to respond to viral infections also diminishes with age as CD8 TCR diversity decreases [65]. Considering the inflammatory microenvironment of aging, we believe that this is a manifestation of a positive immune regulatory function that weakens with aging. Taken together, our findings add weight to the view that the cardiovascular endothelium also has the immunomodulation ability, and that this ability is directly related to a specific class of EC.

Fourthly, we found that there are two types of EC related to angiogenesis in the heart, Proliferating and Angiogenic ECs. This is similar to the “Sprouting angiogenesis model” of blood vessels [66]. By performing a pseudo-temporal analysis of all vascular ECs, we found that Proliferating EC can act as an ‘initiator’ of neovascularization, which is more akin to the ‘sprouting’ process of neovascularization. Angiogenic EC, on the other hand, acts more like an “executor” of differentiation into different EC cells. The overall differentiation trajectory and results are consistent with previous reports [67–69]. Overall, we found that senescence does not significantly alter the differentiation trajectory of neovascularization. However, it significantly impairs the ability to angiogenesis and differentiate of endothelium. This finding offers a deeper understanding of the mechanism of angiogenesis and differentiation of heart vasculature.

Fifthly, we analyze the changes caused by aging on endothelial intercellular communication. The results show that most of the aging ECs falls into a state of signal overshoot. We also analyzed some signaling pathways unique to youth and aging. Finally, further analysis of cell communication between senescent ECs was also carried out.

This study has many limitations. First, we have only performed single-cell RNA analysis of mouse heart endothelium and cannot determine whether the molecular regulatory mechanisms identified in this study are similarly seen in primate or human heart endothelium. Second, we would like to acknowledge that future protein analysis and functional validation experiments are required to confirm the role of each EC phenotype. Third, we removed pericytes (Pdgfrb) from our analysis, which may have removed some of the endothelial cells undergoing EndMT due to the relevance of the PDGF pathway to Aging-EC1. Finally, we cannot exclude the possibility that some EC cells or sub-types may have been lost during tissue dissociation and MACS-based EC enrichment.

Nevertheless, by constructing this single-cell resolution transcriptome atlas of the cardiac endothelium, we have a better

understanding of the physiological aging of the cardiac endothelium and its pathological relevance. This study provides a rich resource for understanding potential diagnostic biomarkers of cardiovascular aging and in the prevention and treatment of age-related cardiovascular disease.

4. Methods

4.1. Animals

Six-to eight-week-old and 48-month-old wild-type C57BL6/J mouse were housed at the Animal Management Center. All animal experimental procedures were in compliance with the legal requirements for animal research.

The Young and Old mouse were processed parallelly, including all baseline information, feeding environment, material retrieval method, quality control of sequencing data, and other pertinent details.

4.2. Collection of cardiac ECs cells

After perfusion with PBS, the mouse hearts were surgically removed, rinsed with ice-cold PBS and dissected into small pieces using sterile scalpels. Then, the tissue was transferred to 10 ml HBSS digestion buffer, including 0.1% collagenase II (Thermo Fisher Scientific, Cat# 17101015), 0.25% collagenase IV (Thermo Fisher Scientific, Cat# 17104019), 7.5 mg/mL DNase I (Sigma-Aldrich, Cat # 11284932001), and incubated in a 37 °C water bath for 25 min, pipetting it with a 1 ml tip every 5 min. 1 ml of 10% FBS (Biological Industries, Cat# 04-001-1A) was used to terminate digestion. The cell suspension is filtered through a 40 mm cell strainer (Sigma-Aldrich, Cat#CLS431750-50 EA) and centrifuged at 300 g for 5 min. Carefully remove the obtained supernatant and then enrich the ECs in the cell suspension using CD31 microbeads (Miltenyi Biotec, Cat#130-097-418) in DMEM medium containing 10% FBS (GIBCO, Cat #C11330500BT) according to the manufacturer's instructions.

4.3. Library preparation and sequencing

We resuspended freshly isolated cardiac ECs in PBS containing 0.04% ultrapure BSA. The scRNA-seq libraries were prepared using Chromium Single Cell 3′ Reagent Kits v2 (10× Genomics; Pleasanton, CA, USA) according to the manufacturer's instructions. The target recovery rate for all libraries was 5000 cells. Generated libraries were sequenced on an Illumina HiSeq4000 and then demultiplexed and mapped to the mouse genome (build mm10) using CellRanger (10× Genomics, version 2.1.1).

4.4. Quality control of scRNA-seq data

Using CellRanger software (10× Genomics), gene expression matrices were generated. The sample data were summarized using CellRanger software and the raw data were analyzed in R (version 4.1.1). Data from young and old cardiac EC samples were logarithmized using Seurat's "LogNormalize" algorithm. With "FindIntegrationAnchors", we selected features and anchor points for downstream integration, ensuring that all cells were counted. The following quality control steps were then performed.

(i) Genes expressed in less than 3 cells or with a line average < 0.002 were not considered.
(ii) Cells expressing less than 200 genes (low quality), and cells expressing more than 4000 genes (potential doublets) were excluded from further analysis.
(iii) Cells with more than 10% of unique molecular identifiers (UMIs) from the mitochondrial genome were excluded.

4.5. Clustering and identification of cell types

We used the seurat3 approach to integrate all the samples. After data integration and scaling, principal component analysis was performed by the "RunPCA" function. Graph-based clustering was then performed with Seurat's "FindClusters" function, which clusters cells according to their gene expression (cluster resolution = 0.25, k-nearest neighbor = 12). The "FindAllMarkers" function was used to determine marker genes for each cluster, and only those with min.pct>0.25 and logfc.threshold>0.25 were considered as marker genes. We screened these top 50 lists of marker genes for each identified cluster to identify consistent enrichment of known canonical marker genes for traditional EC subtypes (i.e., Capillary arterial, Capillary venous, Artery, Vein, Lymphatic) and genes involved in specific cellular pathways or processes to facilitate putative annotation of clusters (i.e. Angiogenic and Proliferating, annotated according to biologically meaningful phenotypes.

4.6. Immunofluorescence staining

We performed immunofluorescence staining as previously described [30]. Briefly, paraffin sections were dewaxed 3 times in xylene and treated with gradient ethanol (100%, 85%, 70%). After waiting for it to cool to room temperature (RT), the slices are rinsed twice in PBS. The slices are soaked in 0.01% pepsin and digested at 37 °C for 10 min. We infiltrated with PBS containing 0.4% Triton X-100 for 2 h and rinse with PBS. We incubated the sections with blocking buffer (PBS containing 5% BSA) for 1 h at RT. The rabbit-derived primary antibody CD31, Mouse Anti-Digoxin Conjugate RNA probe, and Rabbit Anti-Biotin Conjugate RNA probe were subsequently

diluted with 5% BSA at a ratio of 1:1:1:500. We incubated the diluted antibody with the slice overnight at 4 °C. Then Goat Anti-Rabbit AF488, Anti-Biotin FITC-Conjugate and HRP-Monoclonal Mouse Anti-Digoxin Antibody were diluted at RT at a ratio of 1:1:1:500, and incubated with slice for 1 h. Finally, the nucleus is counterstained with DAPI. The Zeiss 980 confocal system is used for immunofluorescence microscopy. All mRNA FISH probes were purchased from the Exonbio Lab (Guangzhou, China). The antibodies and probes used for immunofluorescence staining are as follows: Anti-CD31(Thermo Fisher, PA5-32321,1:500), Apln mRNA FISH Probe (007.220701), Ogn mRNA FISH Probe (007.220702), mus Cd52 mRNA FISH Probe (007.221040), mus Trem11 mRNA FISH Probe (007.221014), mus Birc5 mRNA FISH Probe (007.221012). The secondary antibodies used are as follows: Goat Anti-Rabbit AF488 (Thermo Fisher, A-11008, 1:500), Anti-Biotin FITC-Conjugate (BS–0437P-FITC, Bioss, 1:500) and HRP-Monoclonal Mouse Anti-Digoxin Antibody(200-032-156, Jackson, 1:500).

4.7. Analysis of DEGs between young and old cardiac ECs data

Differential gene expression analysis was performed with Seurat's "FindMarkers" function for the old and young groups using the Wilcox test. Only those with adjusted $|\log FC| > 0.25$ were identified as DEGs.

4.8. GO terminology and KEGG pathway analysis

GO and KEGG pathway enrichment analysis of marker genes and aging-associated DEGs was performed with Metascape (https://metascape.org/gp/index.html). Results were visualized with the ggplot2 R package (https://ggplot2.tidyverse.org/) (version 3.3.5).

4.9. Genome score analysis

The score for each genome was calculated by using the Seurat function "AddModuleScore". Previously published literature was manually analyzed to identify genes associated with procoagulation and SASP [7,70,71]. The genes associated with EMT were from another study [72]. The set of genes associated with inflammation and WNT pathway was from Zhang's study [30]. The gene sets associated with cardiovascular diseases were obtained from the database DisGeNET (https://www.disgenet.org/home/), obtained by filtering for "disease name" (heart failure, atherosclerosis, myocardial infarction, cardiac hypertrophy, coronary artery disease).

4.10. Pseudo-time analysis

Both Monocle and Monocle3 R packages were used for pseudo-temporal analysis. Genes with high variability in the "VariableFeatures" function in the Seurat package were used as ranked genes. Trajectories were constructed using the DDRTree dimensionality reduction method and plotted in two dimensions. DEGs associated with temporal differentiation were obtained with a cut-off of q-value <1e-4.

5. Analysis of transcriptional regulatory networks

Transcriptional regulatory network analysis was performed using the SCENIC workflow (version 1.1.2.2). Cell type-specific transcriptional regulatory networks were calculated by using all genes from young and old cardiac ECs. The obtained transcriptional regulatory networks were visualized by Cytoscape (version 3.8.2) [73].

5.1. Cell-cell communication analysis

Cell-cell communication analysis was conducted using CellChat R package (version 1.1.3) [47]. Analysis and comparison of old and young endothelial cells were performed separately.

Ethics approval

The experiment was approved by the Institutional Animal Ethic Committee Zhongshan Ophthalmic Center, 2020-169.

Author contribution statement

Zhong Liu: Analyzed and interpreted the data; Wrote the paper.
Yanjing Huang: Analyzed and interpreted the data.
Dongliang Wang, Mengke Li, Zhuoxing Shi: Contributed reagents, materials, analysis tools or data.
Qikai Zhang, Caineng Pan, Yuheng Lin, Yuanting Luo: Performed the experiments.
Ping Zhang, Yingfeng Zheng: Conceived and designed the experiments.

Funding statement

This study was funded by the National Natural Science Foundation of China (81721003); the State Key Laboratory of

Ophthalmology, Zhongshan Ophthalmic Center, Sun Yat-sen University, China.

Data availability statement

Data associated with this study has been deposited at National Genomics Data Center under the accession number HRA004465.

Data and code availability

The sequencing data of 10× is stored in NGDC database (National Genomics Data Center) (HRA004465) and all are publicly available at the time of publication. This study did not generate any unique code. SOFTWARE: All software that mentioned in this article is freely or commercially available.

Declaration of competing interest

The authors declare that they have no known competing financial interests or personal relationships that could have appeared to influence the work reported in this paper.

Appendix A. Supplementary data

Supplementary data to this article can be found online at https://doi.org/10.1016/j.heliyon.2023.e18324.

References

[1] V. Obas, R.S. Vasan, The aging heart, Clin. Sci. 132 (13) (2018) 1367–1382, https://doi.org/10.1042/cs20171156.
[2] E.G. Lakatta, D. Levy, Arterial and cardiac aging: major shareholders in cardiovascular disease enterprises, Circulation 107 (1) (2003) 139–146, https://doi.org/10.1161/01.cir.0000048892.83521.58.
[3] Z. Ungvari, S. Tarantini, A.J. Donato, V. Galvan, A. Csiszar, Mechanisms of vascular aging, Circ. Res. 123 (7) (2018) 849–867, https://doi.org/10.1161/circresaha.118.311378.
[4] G. Jia, A.R. Aroor, C. Jia, J.R. Sowers, Endothelial cell senescence in aging-related vascular dysfunction, Biochim. Biophys. Acta (BBA) - Mol. Basis Dis. 1865 (7) (2019) 1802–1809, https://doi.org/10.1016/j.bbadis.2018.08.008.
[5] M. El Assar, J. Angulo, L. Rodríguez-Mañas, Oxidative stress and vascular inflammation in aging, Free Radic. Biol. Med. 65 (2013) 380–401, https://doi.org/10.1016/j.freeradbiomed.2013.07.003.
[6] H.J. Hwang, N. Kim, A.B. Herman, M. Gorospe, J.-S. Lee, Factors and pathways modulating endothelial cell senescence in vascular aging, IJMS 23 (17) (2022) 10135, https://doi.org/10.3390/ijms231710135.
[7] S. Ma, et al., Single-cell transcriptomic atlas of primate cardiopulmonary aging, Cell Res. (2020), https://doi.org/10.1038/s41422-020-00412-6.
[8] T. T. M. Consortium, A single-cell transcriptomic atlas characterizes ageing tissues in the mouse, Nature 583 (7817) (2020) 590–595, https://doi.org/10.1038/s41586-020-2496-1.
[9] J. Kalucka, et al., Single-cell transcriptome atlas of murine endothelial cells, e20, Cell 180 (4) (2020) 764–779, https://doi.org/10.1016/j.cell.2020.01.015.
[10] N.E. Propson, et al., Endothelial C3a receptor mediates vascular inflammation and blood-brain barrier permeability during aging, J. Clin. Invest. 131 (1) (2021), https://doi.org/10.1172/jci140966.
[11] M.J. Végh, et al., Hippocampal extracellular matrix levels and stochasticity in synaptic protein expression increase with age and are associated with age-dependent cognitive decline, Mol. Cell. Proteomics 13 (11) (2014) 2975–2985, https://doi.org/10.1074/mcp.m113.032086.
[12] K. Meyer, T. Patra Vijayamahantesh, R. Ray, SARS-CoV-2 spike protein induces paracrine senescence and leukocyte adhesion in endothelial cells, J. Virol. 95 (no. 17) (2021), https://doi.org/10.1128/jvi.00794-21.
[13] J. Moriya, T. Minamino, Angiogenesis, cancer, and vascular aging, Front. Cardiovasc. Med 4 (2017), https://doi.org/10.3389/fcvm.2017.00065.
[14] Z. Ungvari, et al., Endothelial dysfunction and angiogenesis impairment in the ageing vasculature, Nat. Rev. Cardiol. 15 (9) (2018) 555–565, https://doi.org/10.1038/s41569-018-0030-z.
[15] W. Sendama, The effect of ageing on the resolution of inflammation, Ageing Res. Rev. 57 (2020) 101000, https://doi.org/10.1016/j.arr.2019.101000.
[16] Q. Liu, et al., *SERPINA1* gene expression in whole blood links the rs6647 variant G allele to an increased risk of large artery atherosclerotic stroke, FASEB j 34 (8) (2020) 10107–10116, https://doi.org/10.1096/fj.201903197r.
[17] Y. Li, et al., S100a8/a9 signaling causes mitochondrial dysfunction and cardiomyocyte death in response to ischemic/reperfusion injury, Circulation 140 (9) (2019) 751–764, https://doi.org/10.1161/circulationaha.118.039262.
[18] X. Ren, et al., COVID-19 immune features revealed by a large-scale single-cell transcriptome atlas, Cell 184 (7) (2021) 1895–1913, https://doi.org/10.1016/j.cell.2021.01.053, e19.
[19] F. Penkava, et al., Single-cell sequencing reveals clonal expansions of pro-inflammatory synovial CD8 T cells expressing tissue-homing receptors in psoriatic arthritis, Nat. Commun. 11 (no. 1) (2020), https://doi.org/10.1038/s41467-020-18513-6.
[20] Y. Zhang, et al., Macrophage migration inhibitory factor activates the inflammatory response in joint capsule fibroblasts following post-traumatic joint contracture, Aging 13 (4) (2021) 5804–5823, https://doi.org/10.18632/aging.202505.
[21] K. Contrepois, et al., Histone variant H2A.J accumulates in senescent cells and promotes inflammatory gene expression, Nat. Commun. 8 (no. 1) (2017), https://doi.org/10.1038/ncomms14995.
[22] B.S. Li, A.L. Jin, Z. Zhou, J.H. Seo, B.-M. Choi, DRG2 accelerates senescence via negative regulation of SIRT1 in human diploid fibroblasts, Oxid. Med. Cell. Longev. (2021) 1–16, https://doi.org/10.1155/2021/7301373, 2021.
[23] H. Yousef, et al., Aged blood impairs hippocampal neural precursor activity and activates microglia via brain endothelial cell VCAM1, Nat. Med. 25 (6) (2019) 988–1000, https://doi.org/10.1038/s41591-019-0440-4.
[24] X. Liu, et al., Bmal1 regulates the redox rhythm of HSPB1, and homooxidized HSPB1 attenuates the oxidative stress injury of cardiomyocytes, Oxid. Med. Cell. Longev. (2021) 1–16, https://doi.org/10.1155/2021/5542815, 2021.
[25] Y. Wang, et al., Cardiomyocyte-specific deficiency of HSPB1 worsens cardiac dysfunction by activating NFκB-mediated leucocyte recruitment after myocardial infarction, Cardiovasc. Res. 115 (1) (2018) 154–167, https://doi.org/10.1093/cvr/cvy163.

[26] E. Reichman-Warmusz, M. Brzozowa-Zasada, C. Wojciechowska, D. Dudek, O. Warmusz, R. Wojnicz, "Decreased immunoreactivity of von Willebrand factor may reflect persistent nature of the endothelial dysfunction in non-ischemic heart failure, Folia Histochem. Cytobiol. (2021), https://doi.org/10.5603/fhc.a2021.0012.
[27] M. Braile, et al., "VEGF-A in cardiomyocytes and heart diseases, IJMS 21 (15) (2020) 5294, https://doi.org/10.3390/ijms21155294.
[28] M. Bartekova, J. Radosinska, M. Jelemensky, N.S. Dhalla, "Role of cytokines and inflammation in heart function during health and disease," *Heart Fail Rev*, vol, 23, no 5 (2018) 733–758, https://doi.org/10.1007/s10741-018-9716-x.
[29] J. Birch, J. Gil, Senescence and the SASP: many therapeutic avenues, Genes Dev 34 (no. 23–24) (2020) 1565–1576, https://doi.org/10.1101/gad.343129.120.
[30] H. Zhang, et al., Single-nucleus transcriptomic landscape of primate hippocampal aging, Protein & Cell 9 (2021).
[31] D. Mason, et al., CD79a: a novel marker for B-cell neoplasms in routinely processed tissue samples, Blood 86 (4) (1995) 1453–1459, 10.1182/blood.v86.4.1453.bloodjournal8641453.
[32] S. Keshav, P. Chung, G. Milon, S. Gordon, Lysozyme is an inducible marker of macrophage activation in murine tissues as demonstrated by in situ hybridization, J. Exp. Med 174 (5) (1991) 1049–1058, https://doi.org/10.1084/jem.174.5.1049.
[33] Z. Wu, Z. Zhang, Z. Lei, P. Lei, CD14: biology and role in the pathogenesis of disease, Cytokine Growth Factor Rev. 48 (2019) 24–31, https://doi.org/10.1016/j.cytogfr.2019.06.003.
[34] S. Bhattacharya, et al., ImmPort: disseminating data to the public for the future of immunology, Immunol. Res. 58 (no. 2–3) (2014) 234–239, https://doi.org/10.1007/s12026-014-8516-1.
[35] A. Brauning, et al., Aging of the immune system: focus on natural killer cells phenotype and functions, Cells 11 (6) (2022) 1017, https://doi.org/10.3390/cells11061017.
[36] A.N. Akbar, D.W. Gilroy, "Aging immunity may exacerbate COVID-19," *Science*, vol, 369, no 6501 (2020) 256–257, https://doi.org/10.1126/science.abb0762.
[37] L. Niklason, G. Dai, Arterial venous differentiation for vascular bioengineering, Annu. Rev. Biomed. Eng. 20 (1) (2018) 431–447, https://doi.org/10.1146/annurev-bioeng-062117-121231.
[38] R.S. Apte, D.S. Chen, N. Ferrara, VEGF in signaling and disease: beyond discovery and development, Cell 176 (6) (2019) 1248–1264, https://doi.org/10.1016/j.cell.2019.01.021.
[39] M. Nash, J.P. McGrath, S.P. Cartland, S. Patel, M.M. Kavurma, Tumour necrosis factor superfamily members in ischaemic vascular diseases, Cardiovasc. Res. 115 (4) (2019) 713–720, https://doi.org/10.1093/cvr/cvz042.
[40] D.-Y. Chen, et al., Endothelium-derived semaphorin 3G attenuates ischemic retinopathy by coordinating β-catenin–dependent vascular remodeling, J. Clin. Invest. 131 (no. 4) (2021), https://doi.org/10.1172/jci135296.
[41] H. Li, L. Hou, Regulation of melanocyte stem cell behavior by the niche microenvironment, Pigment Cell Melanoma Res 31 (5) (2018) 556–569, https://doi.org/10.1111/pcmr.12701.
[42] S. Liu, et al., "A role of KIT receptor signaling for proliferation and differentiation of rat stem Leydig cells in vitro, Mol. Cell. Endocrinol. 444 (2017) 1–8, https://doi.org/10.1016/j.mce.2017.01.023.
[43] Z. Su, J. Wang, Q. Lai, H. Zhao, L. Hou, KIT ligand produced by limbal niche cells under control of SOX10 maintains limbal epithelial stem cell survival by activating the KIT/AKT signalling pathway, J. Cell Mol. Med. 24 (20) (2020) 12020–12031, https://doi.org/10.1111/jcmm.15830.
[44] J. Sheng, D. Liu, X. Kang, Y. Chen, K. Jiang, W. Zheng, Egr-1 increases angiogenesis in cartilage via binding Netrin-1 receptor DCC promoter, J. Orthop. Surg. Res. 13 (no. 1) (2018), https://doi.org/10.1186/s13018-018-0826-x.
[45] J. Yan, Y. Gao, S. Lin, Y. Li, L. Shi, Q. Kan, EGR1-CCL2 feedback loop maintains epithelial-mesenchymal transition of cisplatin-resistant gastric cancer cells and promotes tumor angiogenesis, Dig. Dis. Sci. (2021), https://doi.org/10.1007/s10620-021-07250-5.
[46] T. Kanno, et al., JunB promotes cell invasion and angiogenesis in VHL-defective renal cell carcinoma, Oncogene 31 (25) (2011) 3098–3110, https://doi.org/10.1038/onc.2011.475.
[47] S. Jin, et al., Inference and analysis of cell-cell communication using CellChat, Nat. Commun. 12 (no. 1) (2021), https://doi.org/10.1038/s41467-021-21246-9.
[48] H. Scott, P. Brandtzaeg, H. Hirschberg, B.G. Solheim, E. Thorsby, Vascular and renal distribution of HLA-DR-like antigens, Tissue Antigens 18 (3) (1981) 195–202, https://doi.org/10.1111/j.1399-0039.1981.tb01382.x.
[49] D.N.J. Hart, S.V. Fuggle, K.A. Williams, J.W. Fabre, A. Ting, P.J. Morris, Localization of hla-abc and dr antigens in human kidney, Transplantation Journal 31 (6) (1981) 428–433, https://doi.org/10.1097/00007890-198106000-00005.
[50] H. Hirschberg, et al., Antigen-presenting properties of human vascular endothelial cells, The Journal of experimental medicine 152 (2 Pt 2) (1980) 249s–255s.
[51] C.V. Carman, R. Martinelli, T lymphocyte–endothelial interactions: emerging understanding of trafficking and antigen-specific immunity, Front. Immunol. 6 (2015), https://doi.org/10.3389/fimmu.2015.00603.
[52] A. Ager, "High Endothelial Venules, Other Blood, Vessels: critical regulators of lymphoid organ development and function, Front. Immunol. 8 (2017), https://doi.org/10.3389/fimmu.2017.00045.
[53] M. Georganaki, L. van Hooren, A. Dimberg, "Vascular targeting to increase the efficiency of immune checkpoint blockade in cancer, Front. Immunol. 9 (2018), https://doi.org/10.3389/fimmu.2018.03081.
[54] W.A. Muller, Leukocyte-endothelial cell interactions in the inflammatory response, Lab. Invest. 82 (5) (2002) 521–534, https://doi.org/10.1038/labinvest.3780446.
[55] S.W. Kang, et al., Anti-CD137 suppresses tumor growth by blocking reverse signaling by CD137 ligand, Cancer Res. 77 (21) (2017) 5989–6000, https://doi.org/10.1158/0008-5472.can-17-0610.
[56] A. Limmer, et al., Cross-presentation of oral antigens by liver sinusoidal endothelial cells leads to CD8 T cell tolerance, Eur. J. Immunol. 35 (10) (2005) 2970–2981, https://doi.org/10.1002/eji.200526034.
[57] A. Limmer, et al., Efficient presentation of exogenous antigen by liver endothelial cells to CD8+ T cells results in antigen-specific T-cell tolerance, Nat. Med. 6 (12) (2000) 1348–1354, https://doi.org/10.1038/82161.
[58] A. Jambusaria, et al., Endothelial heterogeneity across distinct vascular beds during homeostasis and inflammation, Elife 9 (2020), https://doi.org/10.7554/elife.51413.
[59] A. Gillich, et al., Capillary cell-type specialization in the alveolus, Nature 586 (7831) (2020) 785–789, https://doi.org/10.1038/s41586-020-2822-7.
[60] N.I. Dmitrieva, M.B. Burg, Elevated sodium and dehydration stimulate inflammatory signaling in endothelial cells and promote atherosclerosis, PLoS One 10 (no. 6) (2015), e0128870, https://doi.org/10.1371/journal.pone.0128870.
[61] S.J. Dumas, et al., Single-cell RNA sequencing reveals renal endothelium heterogeneity and metabolic adaptation to water deprivation, JASN (J. Am. Soc. Nephrol.) 31 (1) (2019) 118–138, https://doi.org/10.1681/asn.2019080832.
[62] I. Spadoni, G. Fornasa, M. Rescigno, Organ-specific protection mediated by cooperation between vascular and epithelial barriers, Nat. Rev. Immunol. 17 (12) (2017) 761–773, https://doi.org/10.1038/nri.2017.100.
[63] G.G. Garcia, R.A. Miller, Age-Dependent defects in TCR-triggered cytoskeletal rearrangement in CD4+ T cells, J. Immunol. 169 (9) (2002) 5021–5027, https://doi.org/10.4049/jimmunol.169.9.5021.
[64] L. Haynes, P.-J. Linton, S.M. Eaton, S.L. Tonkonogy, S.L. Swain, Interleukin 2, but not other common γ chain–binding cytokines, can reverse the defect in generation of Cd4 effector T cells from naive T cells of aged mice, J. Exp. Med 190 (7) (1999) 1013–1024, https://doi.org/10.1084/jem.190.7.1013.
[65] E.J. Yager, M. Ahmed, K. Lanzer, T.D. Randall, D.L. Woodland, M.A. Blackman, Age-associated decline in T cell repertoire diversity leads to holes in the repertoire and impaired immunity to influenza virus, J. Exp. Med 205 (3) (2008) 711–723, https://doi.org/10.1084/jem.20071140.
[66] M. Hellström, et al., Dll4 signalling through Notch1 regulates formation of tip cells during angiogenesis, Nature 445 (7129) (2007) 776–780, https://doi.org/10.1038/nature05571.
[67] M. Corada, M.F. Morini, E. Dejana, "Signaling pathways in the specification of arteries and veins, ATVB 34 (11) (2014) 2372–2377, https://doi.org/10.1161/atvbaha.114.303218.

[68] F. Liu, et al., Pathophysiologic role of molecules determining arteriovenous differentiation in adult life, J. Vasc. Res. 57 (5) (2020) 245–253, https://doi.org/10.1159/000507627.
[69] W. Luo, et al., Arterialization requires the timely suppression of cell growth, Nature (2020), https://doi.org/10.1038/s41586-020-3018-x.
[70] S.X. Gu, et al., "Thrombocytopathy and endotheliopathy: crucial contributors to COVID-19 thromboinflammation,", Nat. Rev. Cardiol. (2020) https://doi.org/10.1038/s41569-020-00469-1.
[71] B. Hoppe, T. Dörner, "Coagulation and the fibrin network in rheumatic disease, a role beyond haemostasis," Nat Rev Rheumatol 8 (12) (2012) 738–746, https://doi.org/10.1038/nrrheum.2012.184.
[72] S.V. Vasaikar, et al., EMTome: a resource for pan-cancer analysis of epithelial-mesenchymal transition genes and signatures, Br. J. Cancer 124 (1) (2020) 259–269, https://doi.org/10.1038/s41416-020-01178-9.
[73] P. Shannon, et al., Cytoscape: a software environment for integrated models of biomolecular interaction networks, Genome Res. 13 (11) (2003) 2498–2504, https://doi.org/10.1101/gr.1239303.